MOTION BLUR ESTIMATION OF HANDHELD CAMERA USING REGULAR- AND SHORT-EXPOSURE IMAGE PAIR

Hiroshi Kano, Haruo Hatanaka, Shimpei Fukumoto and Haruhiko Murata

SANYO Electric Co., Ltd., Osaka, Japan

ABSTRACT

We present in this paper a new image stabilization technology to address motion blurs from camera shake with a regular- and short-exposure image pair taken consecutively. The proposed motion estimation process in this technology adopts a Wiener filter to estimate motion blur using few selected feature corresponding points in the image pair. To obtain a more reliable and precise result, a multi-resolution and morphological image processing technique is then used to further refine the initial estimation. This technology has been applied successfully as an image stabilization function on a consumer digital still camera. The resulting performance is 0.7–1.4 EV exposure time step gain with an average processing time of 3.1 seconds for a 6M pixel image.

Index Terms— image restoration, image stabilization, blur kernel, blind deconvolution, digital still camera

1. INTRODUCTION

Image stabilization function is one of the most effective features developed for a digital still camera. There are two general approaches to image stabilization. One is an optical method involving mechanical movements of optical devices such as a lens and an image sensor. The other is an image processing method that compensates the blurred image after capturing the image.

Each method has pros and cons. The image processing method is beneficial from its small stabilization module and low manufacturing cost, because all components except gyro sensors are implemented in the system LSI, DSP and firmware. Moreover if the gyro sensors for motion detection are not necessary, it is a great advantage over the optical method which must rely on the sensors.

A number of studies have been conducted on image deblurring in the past years [1][2][3] and lately some of them have been proposed for application to camera shake correction in digital still cameras [4][5][6][7][8][9]. It is difficult to introduce them into an actual product, because conventional methods produce poor blur kernels and generate ringing artifacts in restored images. The latest methods have improved, however they require a long processing time.

We have developed for a digital still camera a new image stabilization technology that is based on image deconvolution in case of unknown blur, "blind deconvolution", and have reduced processing time. In this paper we describe a newly developed motion blur estimation algorithm and the image stabilization function in which the algorithm has been implemented. Thereupon we present some experimental results.

2. PREVIOUS WORK

Research in blind deconvolution has a long history. None of which has ever been applied to consumer cameras, because it is difficult to compute a stable and precise motion blur in a reasonable time. Blind deconvolution from a single image is most attractive and difficult. Cannon's method [2] assumes straight blur and constant motion speed, however the actual camera shake is complex and the speed is not constant. The iterative method proposed by Ayers [3] is not stable and often converges to a local minimum. Recently, Fergus [4] and Shan [7] proposed more sophisticated methods, yet they are time consuming and difficult to be applied to a digital still camera.

An image pair consisting of a regular-exposure image and a short-exposure image shooting the same scene alleviates the difficulty of estimating the motion blur fundamentally. Lim's method [10] computes a blur kernel from two images by solving a linear least-square equation. Although their method is simple and fast, the blur kernel generated is poor. Yuan [6] proposed a similar and more refined regularization method that consumes much time on iterations. Our method, similar to both of the Lim's method and Yuan's method, is simple and fast and produces blur kernel with quality precise enough to be applicable on a digital still camera.

3. MOTION BLUR ESTIMATION FOR HANDHELD CAMERA

The basis of our algorithm is a Wiener-filter-based estimation. We propose some unique techniques that improve the robustness and precision of this estimation.

3.1. General Principle

A blur kernel operator **k** is assumed to be shift-invariant. Given two images, the blurred image (regular-exposure image) **r** and the blur-less image (short-exposure and gain-up image) **s,** the relation between them can be described as

$$\mathbf{r} = \mathbf{k} \otimes \mathbf{f} + \mathbf{n}_\mathbf{r} \quad (1a)$$

$$\mathbf{s} = \mathbf{f} + \mathbf{n}_\mathbf{s} \quad (1b)$$

where **f** is an ideal blur-less and noise-less image, $\mathbf{n}_\mathbf{r}$ and $\mathbf{n}_\mathbf{s}$ are noises and $\otimes$ is a convolution operator. From equation (1), we substitute (1b) into **f** in (1a) to obtain

$$\mathbf{r} = \mathbf{k} \otimes \mathbf{s} + \mathbf{n} \quad (2)$$

where

$$\mathbf{n} = \mathbf{n}_\mathbf{r} - \mathbf{k} \otimes \mathbf{n}_\mathbf{s}$$

Here, the two noise terms $\mathbf{n}_\mathbf{r}$ and $\mathbf{n}_\mathbf{s}$ are represented collectively as **n**. In frequency domain, the above equation becomes equation (3).

$$\mathbf{R} = \mathbf{K} \cdot \mathbf{S} + \mathbf{N} \quad (3)$$

R, **K**, **S** and **N** correspond to the Fourier transforms of **r**, **k**, **s** and **n**, respectively. There are several methods to compute $\hat{\mathbf{k}}$, an estimate of **k,** from **r** and **s**. The Wiener filter is optimal in the sense that the average squared error between $\hat{\mathbf{k}}$ and **k** is minimal. The Wiener filter theory gives $\hat{\mathbf{k}}$ as described in equation (4).

$$\hat{\mathbf{k}} = \mathrm{F}^{-1}\left(\frac{\mathbf{R} \cdot \mathbf{S}^*}{\mathbf{S} \cdot \mathbf{S}^* + \Gamma_1} \right) \quad (4)$$

In (4), $\mathbf{S}^*$ is the complex conjugate of **S**. Γ_1 is a constant determined by the ratio between the power spectrum densities of the ideal image and noise. F^{-1} is the inverse Fourier transform.

Image restoration is the process to compute the blur-less image from the blurred image using the estimated blur kernel. Wiener filter, which is different from the previously described, is also a representative method to estimate the blur-less image $\hat{\mathbf{s}}$ given by equation (5).

$$\hat{\mathbf{s}} = \mathrm{F}^{-1}\left(\frac{\mathbf{R} \cdot \hat{\mathbf{K}}^*}{\hat{\mathbf{K}} \cdot \hat{\mathbf{K}}^* + \Gamma_2} \right) \quad (5)$$

Here, $\hat{\mathbf{K}}$ is the Fourier transform of $\hat{\mathbf{k}}$ and Γ_2 is a constant.

There are several constraints that should be considered when applying image restoration techniques to image stabilization on a digital still camera. Since heavy frequency domain processing requires a special hardware, the amount of frequency domain computation should be limited such that the firmware can handle. Also, real time response is often an essential condition for a consumer application. In the case of digital cameras, the permissible limit is a few seconds. Hence linear methods such as the Wiener filter are preferable over iterative methods. And we use spatial domain filtering to restore the blur-less image.

Straightforward implementation of the idea from this section would not be practical due to long processing time and imprecise blur kernel with high noise. We solve the difficulties by developing two techniques. The first is to limit the blur estimation to areas containing distinctive features. The second technique is the refinement of the blur kernel by multi-resolution and morphological image processing. We explain these techniques in the two sections below.

3.2. Motion Blur Estimation Using Feature Points

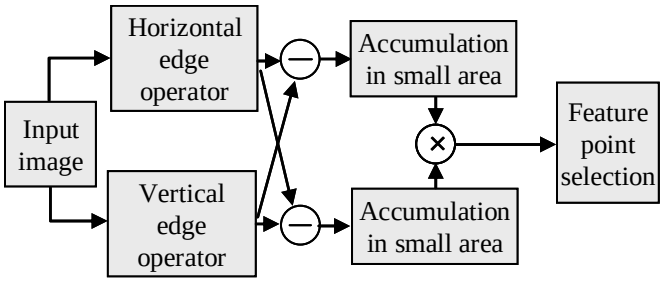

Fig. 1 Feature point detection process

A feature point is a small area containing substantial signal variations along two directions so that the point can be localized precisely [11]. Fig. 1 shows the proposed feature point detection method. Horizontal edge intensity and vertical edge intensity are computed from the input. After the noisy components are filtered out by accumulating the intensity values around a small window, the noise-filtered edge intensity images are multiplied. Feature points are pixels that have high values in the multiplied image. In Fig. 1, an edge intensity of a different direction is subtracted before the accumulation so that the edge intensity for a diagonal edge is not accumulated.

Upon selection of several feature points in the reduced-size short-exposure image, their corresponding points are searched in the reduced-size long-exposure image with a block matching method. The area of the feature point is small such as 8 pixels by 8 pixels. The minimal area necessary for computing a blur kernel depends on the maximum size of the camera shake. If a size of 64 pixels by 64 pixels is used for the blur kernel considering actual sizes of camera shake on the image plane, the size of the image patches for computing the blur kernel becomes the same accordingly. Each image patch is set so that it surrounds one of the selected feature points.

If m corresponding image patches are selected, m equations described as (5) is obtained.

$$\mathbf{r}_i = \mathbf{k} \otimes \mathbf{s}_i + \mathbf{n}_i \ , (i = 1,\ldots,m) \qquad (6)$$

$\mathbf{s}_i$ is the i-th image patch on the short-exposure image. $\mathbf{r}_i$ is the corresponding patch on the regular-exposure image. $\mathbf{k}$ is the blur kernel and $\mathbf{n}_i$ is noise, After the m equations are transformed to the frequency domain and grouped as vectors, equation (6) is rewritten as equation (7).

$$\begin{pmatrix} \mathbf{R}_1 \\ \mathbf{R}_2 \\ \cdots \\ \mathbf{R}_m \end{pmatrix} = \mathbf{K} \cdot \begin{pmatrix} \mathbf{S}_1 \\ \mathbf{S}_2 \\ \cdots \\ \mathbf{S}_m \end{pmatrix} + \begin{pmatrix} \mathbf{N}_1 \\ \mathbf{N}_2 \\ \cdots \\ \mathbf{N}_m \end{pmatrix} \qquad (7)$$

$\mathbf{R}_i$, $\mathbf{S}_i$ and $\mathbf{N}_i$ are the Fourier transforms of $\mathbf{r}_i$, $\mathbf{s}_i$ and $\mathbf{n}_i$, respectively. When $[\mathbf{R}_1,\mathbf{R}_2,\ldots,\mathbf{R}_m]^t$, $[\mathbf{S}_1,\mathbf{S}_2,\ldots,\mathbf{S}_m]^t$ and $[\mathbf{N}_1,\mathbf{N}_2,\ldots,\mathbf{N}_m]^t$ are substituted with $\mathbf{R}$, $\mathbf{S}$ and $\mathbf{N}$, respectively, equation (7) becomes equation (3). Consequently, $\hat{\mathbf{k}}$, the estimate of the blur kernel $\mathbf{k}$, is obtained by equation (4).

The estimation process is fast, because the size of the image patches is small, and typically only four pairs of image patches are used. It is also robust and precise, because distinctive feature points are used.

3.3. Refinement by Multi-resolution and Morphological Image Processing

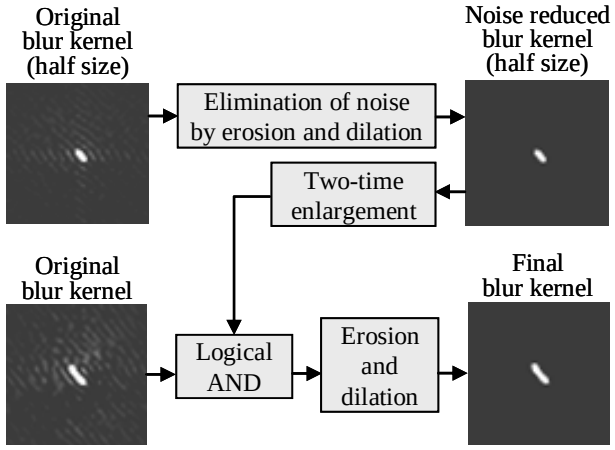

Fig. 2 Refinement of blur kernel

The blur kernel estimated by the procedure described in 3.2 is further refined by a multi-resolution and morphological image process shown in Fig. 2. An original half-size blur kernel estimated with half-size image patches shows small noisy components around a clear blur trace. The noisy components should be eliminated because the true kernel consists of a single trace. We adopt erosion and dilation operations, which are the typical morphological image processing techniques [12], to delete isolated pixels. The half-size noise-reduced blur kernel is enlarged and used as a mask for an original-size blur kernel. The masked blur kernel is further refined by the erosion and dilation operations again.

4. EXPERIMENTAL RESULTS

We have evaluated the performance of the motion blur estimation algorithm and the image stabilization function.

4.1. Blur Kernel Estimation Performance

Table 1 Comparison of estimation performance

	Conventional	Proposed
Success ratio	56 %	96 %
Processing time(PC)	30 sec	0.3 sec
Processing	-	2.4 sec

(PC:Pentium4, 3.2GHz, DSP:90MHz)

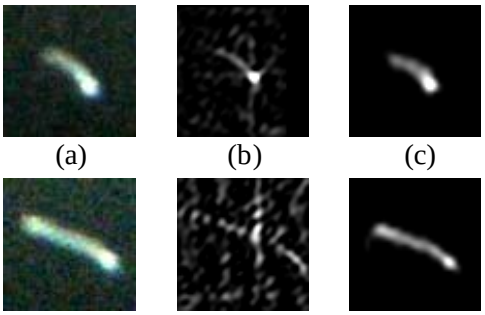

Fig. 3 Examples of estimated PSF: (a) Real PSF of blurred image (size:30x26), (b) Conventional method (success), (c) Proposed method (success), (d) Real PSF of blurred image (size:53x30), (e) Conventional method (failure), (f) Proposed method (success)

Tests were conducted for 1/15 second exposure time and focal length of 105 mm (35mm equivalent). We placed a board with a dotted pattern in front of a resolution chart and took 100 pictures of them. After which, we evaluated the results of both the Ayers' method and our double-exposure-based method. Table 1 shows their success ratios and processing times. Not only the processing time has become 100 times shorter but the success ratio has also improved by 40%.

Two examples of estimated PSF are shown in Fig. 3. We judged that the estimated PSF was a success, if its shape and size were the same as the real PSF by visual inspection.

4.2. Deblurring Performance

The total performance of image stabilization is evaluated by using a prototype camera in which the image stabilizer is implemented. The evaluation method is original and involves calculating MTF (Modulation Transform Function),

which characterizes the sharpness of the image [13]. Table 2 shows a part of the results. We concluded that it is possible to take pictures with a 0.7–1.4 EV longer exposure time step while maintaining the same amount of blur in the 1/125–1/8 second exposure time range. Finally, we present the restored images and estimated PSF using the image stabilizer in Fig. 4.

Table 2 Deblurring performance in exposure time step gain

Exposure time (sec)	ISO Sensitivity		
	100	400	1600
1/15	1.37	1.19	0.94
1/60	1.17	1.26	2.10

(a) Original image with blur (b) Restored image

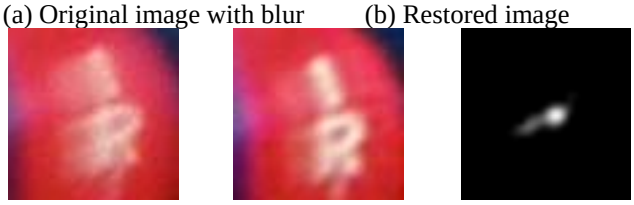

(c) A part of Original Image (d) A part of Restored Image (e) Estimated PSF

Fig. 4 Example image and estimated PSF with proposed method. (Estimated PSF size : 26x18)

5. CONCLUSION

We have developed a new image stabilization technology based on blind deconvolution and implemented it in a digital still camera. Evaluation results show that in the 1/125–1/8 second exposure time range we have achieved a 0.7–1.4 EV exposure time step gain while reducing the processing time to 3.1 seconds on average. Fig. 5 shows a photo of the prototype camera and its specifications.

Imager	1/2.5" CCD, 8M
Lens	3x Zoom
CPU	100MHz
DSP	90MHz, 16bit
Memory	3MB for Deblurring

Fig. 5 Digital still camera with proposed image stabilization function

REFERENCES

[1] M.R. Banham, and A.K. Kataggleos, "Digital Image Restoration," IEEE Signal Processing Magazine, pp. 24-41, 1997.

[2] T.M. Cannon, "Blind Deconvolution of Spatially Invariant Image Blurs With Phase," IEEE Trans. Acoustics, Speech, and Signal Processing, Vol. 24, pp. 58-63, 1976.

[3] G.R. Ayers, and J.C. Dainty, "Iterative blind deconvolution method and its applications," Optics Letters, vol. 13(7), pp. 547-549, July 1988.

[4] R. Fergus, B. Singh, A. Hertzmann, S.T. Roweis, and W. T. Freeman, "Removing Camera Shake from a Single Photograph," ACM Trans. on Graphics, Vol. 25, No.3, pp.787-794, 2006.

[5] L. Yuan, J. Sun, L. Quan, and H.Y. Shum, "Image Deblurring with Blurred/Noisy Image Pairs," ACM Trans. on Graphics, Vol. 26, No.3, Article 1, 2007.

[6] L. Yuan, J. Sun, L. Quan, and H.Y. Shum, "Progressive Inter-scale and Intra-scale Non-blind Image Deconvolution," ACM Trans. on Graphics, Vol. 27, No.3, Article 74, 2008.

[7] Q. Shan, J. Jia, A. Agarwala, "High-quality Deblurring from a Single Image," ACM Trans. on Graphics, Vol. 27, No.3, Article 34, 2008.

[8] A. Levin, Y. Weiss, F. Durand, W. T. Freeman, "Understanding and evaluating blind deconvolution algorithms," Technical report, MIT-CSAIL-TR-2009-014, 2009.

[9] Lu Yuan, Jian Sun, Long Quan and Heung-Yeung Shum, "Blurred/Non-Blurred Image Alignment using Kernel Sparseness Prior," Proc. IEEE ICCV2007, pp.1-8, 2007.

[10] S.H. Lim, and D.A. Silverstein, "Method for Deblurring an Image," US Patent Application, Pub. No. US2006/0187308 A1, Aug 24, 2006.

[11] J. Shi, and C. Tomasi, "Good Features to Track," Proc. IEEE CVPR94, pp.593-600, 1994.

[12] R.C. Gonzalez, and R.E. Woods, "Digital Image Processing," Third Edition, Peason Education, Inc., 2008.

[13] H. Hatanaka, S. Fukumoto, H. Kano, and H. Murata, "An Image Stabilization Technology for Digital Still Camera Based on Blind Deconvolution," IEEE Int. Conf. Consumer Electronics, Tech. Paper 4.3-1, 2009.